2013 IEEE/RSJ International Conference on
Intelligent Robots and Systems (IROS)
November 3-7, 2013. Tokyo, Japan

Functional Analysis of Grasping Motion

Wei Dai, Yu Sun, and Xiaoning Qian

Abstract— **This paper presents a novel grasping motion analysis technique based on functional principal component analysis (fPCA). The functional analysis of grasping motion provides an effective representation of grasping motion and emphasizes motion dynamic features that are omitted by classic PCA-based approaches. The proposed approach represents, processes, and compares grasping motion trajectories in a low-dimensional space. An experiment was conducted to record grasping motion trajectories of 15 different grasp types in Cutkosky grasp taxonomy. We implemented our method for the analysis of collected grasping motion in the PCA+fPCA space, which generated a new data-driven taxonomy of the grasp types, and naturally clustered grasping motion into 5 consistent groups across 5 different subjects. The robustness of the grouping was evaluated and confirmed using a ten-fold cross validation approach.**

I. INTRODUCTION

In Learning from Demonstration (LfD), mapping between humans and robots is one of crucial problems to resolve for successfully transferring skills learned from humans to robots. Grasp classification approaches have been developed to avoid direct kinematic mapping, in which human grasps are classified into different grasp types and a demonstrated grasp is recognized as one of the trained grasp types. Many of the grasp types are defined by the Cutkosky grasp taxonomy, which classifies common human grasps into 16 types based on task requirements and dexterities [1].

A human hand has 22 degrees of freedom (DOF) [2], and classifying a grasp type represented with all the joint variables in a hand is a high-dimensional problem. Fortunately, the motions of finger joints are not entirely independent of each other [3]. Some of the correlations arise from the musculoskeletal architecture [4], in that some finger muscles have insertions on more than one finger, while others have contributions from neural constraints because of linkages in the activation of individual finger muscles [5], [6].

An early attempt to simplify the formula of grasping can be tracked back to Napier (1956) [7], who defined two distinct patterns of movement – precision grip and power grip. Later, more detailed grasp classification was introduced by many researchers [8], [9], [10], [11], [1]. With similar consideration, the Iberall group introduced the concept of "virtual fingers" [12], in which each virtual finger represents all of the fingers that are controlled as one unit in a grasping process.

Santello et al. [13] studied the static hand grasping postures during grasping using a large number of familiar objects and found that the 15 joint angles of the fingers and the thumbs are mostly correlated and that two components could account for $> 80\%$ of the variance between different static hand postures. Thakur et al. [14] used a principal component analysis (PCA) approach to analyze hand posture data obtained from a motion capture system and then defined a set of hand synergies that would describe a generalized grasping motion.

In robotics, researchers recently have been able to use PCA to reduce high dimensional grasping data to a lower dimensional space so that a grasping process is easy to model for learning and control. Ciocarlie and Allen [15] showed the computational advantages of using a reduced dimensionality to control grasping, in which the pre-grasp posture of a robotic hand was derived in the reduced dimension. Peters and Jenkins [16] compared a number of dimensionality reduction approaches that extract two-dimensional manifolds from human demonstration datasets.

Most hand motion analysis approaches are based on PCA or linear discriminant analysis (LDA) that treat the postures in a grasping process as discrete points scattered in a high-dimensional space. The obtained principal components represent the dominant variation directions between hand poses as they are static. However, since the temporal information related to the poses is not preserved or used, the motion feature of the grasping process cannot be fully characterized with PCA. The popular Gaussian mixture model (GMM) treats motion samples as static points, loses the dynamic features of the motion, and then invents artificial dynamics when generating desired robot motions with Gaussian mixture regression (GMR). It loses and distorts the natural motion dynamic features – relative velocity and acceleration, in the tool and the dynamics in the hand-tool interaction. To preserve the dynamics in the motion, we propose to model the motion sequence based on functional principal component analysis (fPCA).

Neither humans nor robots perform a grasping task in a discrete manner. Instead, grasping processes are usually highly continuous and featured with dynamics (velocity and acceleration). To fully model grasping processes and grasp synergy, we need to find a functional-based analysis to preserve temporal and dynamic information. Furthermore, if we wish to control a robot to reproduce a human-like grasping model, it is necessary to control the robot's hand motion with human-like trajectories.

A number of approaches have been developed to recover temporal information from a recorded dataset after PCA and to generate novel trajectories by mapping the recorded trajectories for control. For example, Aleotti and Caselli [17]

Wei Dai, Yu Sun, and Xiaoning Qian are with the Department of Computer Science and Engineering, University of South Florida, Tampa, Florida 33620. yusun@cse.usf.edu

developed a NURBS-based approach to replicate different grasping motion based on the recorded trajectories and postures obtained with a Cyberglove. PCA has also been widely used in biomechanics to describe continuous waveforms [21]. Soechting and Flanders [2] studied the degrees of freedom during typing and found temporal patterns of motion with two to four principal components (PCs) that were computed as a linear combination of the 121 original recorded motion waveforms. In robotics, [18] used Hidden Markov models to recognize grasp types from the taxonomy based on an entire grasp sequence, particularly emphasizing the approaching state. A recent paper [19] analyzed grasping motion by first reducing the high-dimensionality of motion trajectories onto three-dimensional space and preserving the locality of the nonlinear structure in the trajectories by using locality preserving projections (LPP). Then, a Hausdorff distance was used to measure the similarity between trajectories and classify the trajectories into different types in the reduced low-dimensional space.

A new set of statistical techniques, functional data analysis, recently was formulated and used to analyze temporal data [22]. Specifically, functional PCA (fPCA) can be used in motion analysis to extract orthogonal functional principal components (fPCs) from observed motion data without any discretization process and then reduce the dimensionality of the representation for the motion of interest by a linear combination of these fPCs.

In this paper, we explore a novel grasp type grouping and classification approach based on fPCA to recognize and analyze human grasping motion. Different from previous grasping motion analysis using traditional PCA to obtain "eigengrasps" for static hand posture variability, our fPCA-based grasping motion analysis focuses on the temporal relationships between hand postures at each time point from a dynamic perspective. We are interested in the variability range of grasping motion dynamics across different objects and subjects. Specifically, we implement fPCA to capture the principal modes of grasping motion dynamics, which can further be used to learn grasping motion from a human to program robotic hands by demonstration.

II. Principal Motion Extraction

A. Motion feature segmentation and alignment

To compare different trajectories taken in different trials by different subjects, they should be properly aligned to remove temporal artifacts. We first adopt dynamic time warping (DTW) [23], which has been used in matching time series such as speech recognition and economics, to optimally align grasping motion curves that may vary in time between two trials of finger joint displacement sequences by non-linear transformation. The DTW is basically a dynamic programming algorithm which first computes a local-match matrix to store the distances between two trajectories for each time point, and then finds the path that has a minimal overall value within the matrix while satisfying three conditions: boundary condition, monotonicity condition, and step-size condition. The boundary condition makes sure that the path starts at the first point of the aligned sequences and ends at the last point of the aligned sequences. The monotonicity condition makes sure that the aligned trial preserves time-ordering of the original data. In the end, DTW allows us to align different trials of grasps pair-wisely by changing the time step between each frame of the motion records yet reserve motion dynamics in the original records. For example, Figure 1 shows the original five trials of the motions of the thumb-index finger abduction joint D1-D2 MP (top figure) during one type of object grasping task and the same set of curves (bottom figure) after DTW.

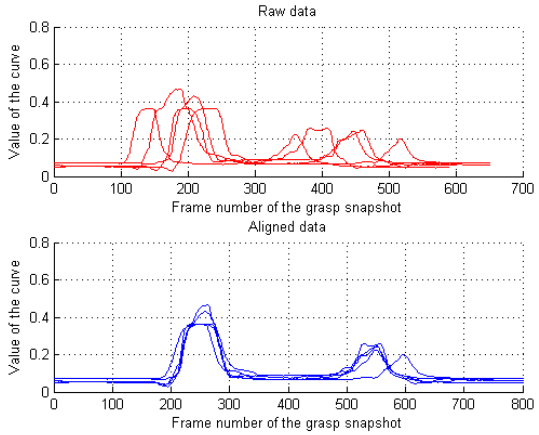

Fig. 1. Top graph shows the original curves; Bottom one shows curves after applying the dynamic time warping. The number of diagonal steps allowed is 20 and the max horizontal or vertical transition in the warping is 10.

B. Principal Motion Extraction for 1-DOF Motion

First, we apply the fPCA approach to a set of 1-DOF joint trajectory data to describe how to compute fPCs and fPCA scores and how to analyze grasping motion in the fPCA space. After alignment, a set of collected 1-DOF joint trajectory data $\mathbf{x}_i(t)$, $i = 1, \ldots, N$ have a common set of sample time points $t_1, \ldots, t_m$, where N is the total number of collected motion trajectories or trials corresponding to different motion types such as grasping of different objects.

Since the datasets of grasping trajectories are currently represented in a discrete form, we first create functional objects to replace the sampled motion data vectors for analysis. In our experiments, we have used B-spline functions as function bases to create the functional objects from the sampled motion data. As the observed grasping motion is not periodical, we consider that these data are all open-ended data and choose spline functions to approximate the underlying grasping functions. The underlying function $\mathbf{x}_i(t)$ is often declared to be smooth. We use a relatively large number of bases to compensate for the penalty introduced by smoothing these functions. In our experiments, we have obtained satisfactory results with dozens of B-spline base functions.

The penalty is quantified by the second derivative $[D^2\mathbf{x}(t)]^2$ at t, which represents the function's *curvature*.

The natural measure of these functions' roughness is the integrated squared second derivative. As a result, the underlying function is the smoothest twice-differentiable curve that fits the motion data. We take uniform time intervals since we treat each measurement equally, which means that we do not segment the motion of the whole grasping procedure. All motion curves are fitted with B-spline function bases, which has L subintervals separated by τ_l, $l = 1, \ldots, L-1$ called knots. The notation $B_k(t, \tau)$ indicates the value sampled at t of the corresponding B-spline basis defined by the knot sequence τ. According to this, we can represent any grasping curve as

$$S(t) = \sum_{k=1}^{L-1} c_k B_k(t, \tau), \tag{1}$$

Assuming that we work with normalized data with zero mean without loss of generality (the mean function can be subtracted from the projected data), we define the covariance function of the projected data as

$$v(s,t) = (N-1)^{-1} \sum y_i(s) y_i(t), \tag{2}$$

where $y_i(s)$ represents the functional objects for the 1-D motion data for the ith trial. With that, the fPCs for fPCA are simply the eigenfunctions of the covariance function:

$$\int v(s,t)\xi_\ell(t)\mathrm{d}t = \rho_\ell \xi_\ell(s), \tag{3}$$

in which ρ_ℓ is the eigenvalue, while $\xi_\ell(t)$ is an corresponding eigenfunction. With the function basis expansion, the system can be solved similarly as in traditional PCA to look for orthonormal eigenfunctions $\xi_\ell(t)$, $\ell = 1, \ldots, L$ whose linear combinations maximize the variation in the data defined by the principal scores using the inner product:

$$\rho_\ell(y_i) = \int \xi_\ell(t) y_i(t) \mathrm{d}t. \tag{4}$$

The fPCs of grasping motion simply represent the principal curves that summarize the angle variation of each DOF through the whole grasping procedure. Figure 2 shows the original curve of the D1 - D2 MP joint (between thumb and index finger) and its first two principal curves (fPCs), which dominate the variation during the grasping motion. Figure 2(c) and (d) show the original trajectory and the reconstructed trajectory using the two fPCs. We can see that the motion is reconstructed without losing much information.

C. Principal Motion Extraction for high-DOF Motions

Ideally, we would like to directly apply fPCA to capture complete functional correlation between these motion functions and identify essential motion patterns from the data to control robots for grasping different objects. However, due to increasing complexity of variance-covariance structure, fPCA is typically limited to the study of the samples of a single function with extension to joint analysis of two functions, meaning that the analysis is done within the sampled curves from the function of one or two variables. In the current study, we take an alternative route to find principal modes of

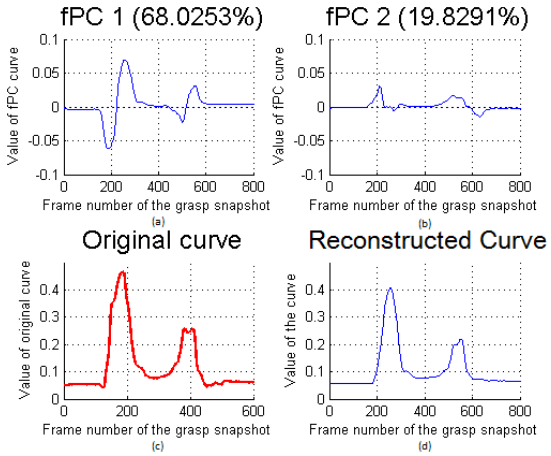

Fig. 2. (a) The most significant fPC that represent the angle variation through grasping procedure. The percentage of variance covered over the mean function is shown in the subtitle. (b) The second significant fPC. (c) The original curve in red solid line. (d) The reconstructed curve using first two fPCs in blue solid line. These data are from the first trial of the large diameter grasping task.

functional dynamics of grasping motion. Instead of directly implementing fPCA to the sampled motion functional data, we first implement a traditional multivariate PCA to extract the principal postures, similar as "eigengrasps" in [15], which capture the major range of hand posture changes across subjects and objects. To do that, we aggregate the sampled motion data $\mathbf{x}_i(t)$ at $t_1, \ldots, t_m$ along time t_l into a data matrix $\mathbf{X} = (x_{jl})$, where $l = 1, \ldots, N \times m$ is the combined index based on trials and sample time points and j is still the index for functional variables. With $\mathbf{X}$, traditional PCA [25] can be implemented to compute principal components as principal postures whose standardized linear combinations span the space with the maximum variance of the data and cover the main variability of hand posture changes. These principal components are the eigenvectors of the covariance matrix $\frac{\mathbf{X}\mathbf{X}^T}{Nm-1}$ with column centered $\mathbf{X}$ without loss of generality. We denote them as $\mathbf{p}_k$, $k = 1, \ldots, K$ with K as the number of principal postures.

With the principal components, we implement fPCA to analyze their temporal functional dynamics by projecting the original sampled motion data to each selected principal component $\mathbf{p}_k$. For each motion along the principal axis, the fPCA in the previous section can be applied. For example, for a 14-DOF time series motion data set, if we select the first three principal components as principal postures by PCA, and then select the first two functional principal components with fPCA, we can represent a 14-DOF motion trajectory with six variables. Basically, we can represent and compare the 14-DOF trajectories in the motion dataset in a six-dimensional space after PCA-fPCA analysis.

III. Experiment Design and Data Collection

We captured the hand motion in joint angles with a right-handed 5DT DataGlove 14 Ultra that records 14 joints of a hand using a series of optical fibers. Figure 3 shows a photograph of the dataglove side by side with a schematic

drawing of the joints' motion being captured [24]. The sampling rate of 5DT DataGlove 14 Ultra is 62.5Hz. Five subjects have participated during the data collection, whose heights are between 5 feet 8 inches and 6 feet. We have collected a set of grasping motion data for 9 typical objects for 15 different grasp types by the 5 subjects using a right-handed 5DT DataGlove 14 Ultra. With K-means clustering approach, we are able to generate a data-driven hierarchical grasping taxonomy and recognize grasp types robustly in the fPCA space.

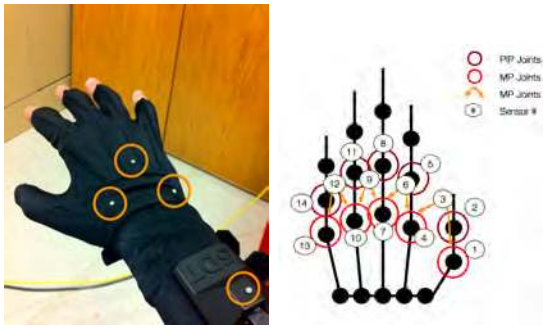

(a) (b)

Fig. 3. (a) The 5DT DataGlove used in our experiment; (b) the measured joints on the right hand and their indices in the DataGlove.

The 15 sets of 14-DOF finger motions were recorded for 5 trials of grasping processes of a total of 9 objects, with the dataglove at the side to indicate the sizes of the objects: spray can, metal tube, screwdriver, tomato, duct tape roll, golf ball, flat tool box, marker, and flat thin plastic (Figure 4). These are daily living objects and were selected to reflect the representative grasps in Cutkosky grasp taxonomy.

Fig. 4. Grasping objects.

IV. Grasping Motion Analysis

The recorded 14-DOF motion data from 5 trials of all 15 grasp types gave a total of 75 14-DOF sampled motion functional trajectories for each subject. With classical PCA, we reduced the DOF of the hand from 14 to 3 by finding 3 principal components as principal hand postures and representing the static grasp postures using PC scores along these principal components. At this point, the motion data were reduced to 75 3-DOF motion trajectories – we computed the three PC scores for every time point of each grasping motion during the grasping procedure. For each dimension in the 3D PCA space, the fPCA was applied to process the 75 motion trajectories to find a set of fPCs that can represent the basic functional dynamics of the trajectories. After the fPCA, each of the original 75 14-DOF motion functions can be represented using 6 independent variables.

The PCA is a good method for extracting information from related empirical variables. Each orthogonal principal component linearly combines the empirical variables with the highest level of variance contribution on that dimension. The variables that have a significant contribution on each component are said to be correlated by their level of variability. Computed with our training data, the first three components cover 83% of the overall variance of the entire data set. Therefore, we chose the first three principal components (PCs) to represent the grasp poses.

Once the principal postures of the grasping data are extracted, analysis continues by evaluating the dynamics of these components. As explained before, the advantages of fPCA reside in the description of the dataset on a temporal graph as a function of time. It relates the correlation of empirical variables throughout the whole motion instead of individual snapshots. We implemented fPCA to analyze the temporal functional dynamics of grasping motion by projecting the original sampled motion data to the vectors corresponding to individual principal postures. In fPCA, we used B-spline functions as our function bases to create the functional objects from the sampled motion data, as the observed grasping motion is not periodical.

Figures 5 and 6 show the eigenfunctions and how they vary over the mean function. In the top graphs, the black line refers to the mean function of the first principal component obtained from the PCA procedure; similarly, the bottom graphs show the second component's mean function. The dashed and point-dashed blue lines describe the first and second component variability over the mean based on derived eigenfunctions.

Similarly, since the first two fPCs for each PC contribute around 95% of the dynamic change in the motion trajectories, we selected them to represent the motion functions. Therefore, each 14-DOF motion trajectory can be first projected on the three PCs to produce a 3-DOF trajectory and then projected in the two fPCs for each of the three PCs. In the end, every grasping motion can be represented with six variables that capture both the static and dynamic features of the motion.

In the six-dimensional space, we applied the K-means clustering algorithm on the grasping trajectories with incremental $k = 2, 3, \ldots, 13$ to find natural grouping of grasp types for different levels. With increasing k, coarse grasp type groups were split to subgroups consistently across the five subjects (Table I), which revealed potential hierarchical taxonomy in the grasping types. The K-means clustering was performed on all 5 subjects individually for 5 trials of 9 different objects with 15 different grasp types according to Cutkosky grasp taxonomy. Figure 8 shows the hierarchy structure of the grasping types obtained for one subject.

By comparing the hierarchy taxonomy from different subjects, we found that the hierarchical taxonomies were the

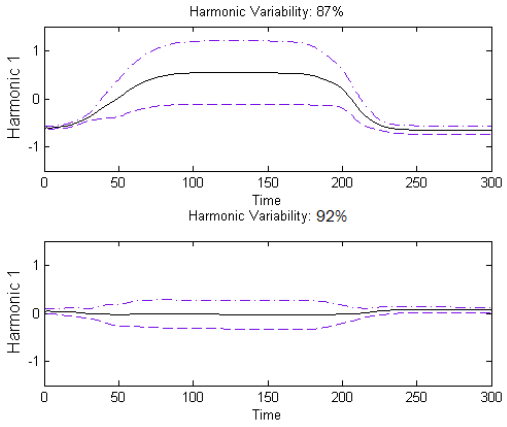

Fig. 5. The first fPC along the first and the second PC over the mean function

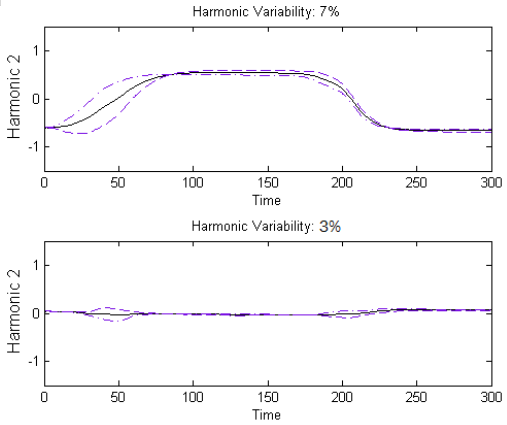

Fig. 6. The second fPC of the first and the second PC over the mean function.

same for all the subjects when $k <= 4$, and then varied from subject to subject after more refined clustering. This indicates that the 15 grasping types can be naturally and stably grouped into 4 types (excluding platform) from the grasping motion point of view. More refined classification did not yield consistent results across subjects since subjects' hands are different and their grasping habits are also different. For comparison, Cutkosky grasp taxonomy is shown in Figure 7. To be consistent, we also included the non-prehensile in the taxonomy, but we did not perform K-means with non-prehensile data since it is not a grasping.

In additional to the non-prehensile that is considered as one group, Group 1 = {platform}. The four grouped grasp types from the grasping trajectories are:

- Group 2 = {Lateal Pinch, Power Disk, Light Tool}
- Group 3 = {Power Sphere, Precision Disk, Thumb-4, Thumb-3, Large Diameter}
- Group 4 = {Small Diameter Adducted Thumb Medium Wrap}
- Group 5 = {Tripod Thumb-2 Thumb-Index}

We further evaluated the robustness of the four grasping groups and the non-prehensile and used the groups to recognize new unseen grasps. First, we randomly split all the collected trials for all the objects to training data set and testing data set and carried out a 10-fold cross validation. Our method achieved a 97.24% recognition rate (confusion matrix is shown in Figure 9a). Then, we used the same set of objects for training and testing. Three of the five trials of each object were used as training data; the remaining two were used as test data. The recognition rate was 99.05% and the confusion matrix is shown in Figure 9b. Last, we randomly selected one of the 15 objects as an unseen object for evaluation, and used the rest for training and cross-validated the objects for 10 times. The recognition rate dropped to 89.16% and the confusion matrix is shown in Figure 9c.

By examining the confusion matrices in Figure 9, we can see that several grasp types were misclassified in the testing process. For instance, the grasp type "Thumb-3," which should be in class 3, was misclassified as class 5 because the variance covered by the interphalangeal joint of the ring finger was very low. This can be seen in Figure 9a. The "Large Diameter," which should be in class 3, was misclassified with "Platform" in class 1. This can be seen in Figure 9b and Figure 9c.

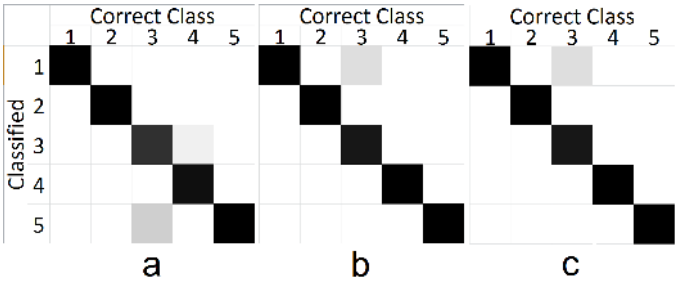

Fig. 9. (a) Confusion matrix for 10-fold cross validation (b) confusion matrix for individual user and seen objects (c) confusion matrix for individual user and unseen objects.

V. CONCLUSIONS AND FUTURE WORKS

We have introduced a new PCA + fPCA-based grasping motion analysis approach that captures correlations among hand joints and represents dynamic features of grasping motion with a low number of variables. The combination of classical components from PCA considered as functional objects for fPCA allows us to process 15 different grasp types in Cutkosky grasp taxonomy in terms of grasping trajectories, to generate a new data-driven taxonomy of the grasp types, and to naturally group them into 5 consistent groups. The results agree with common empirical observations that classify objects based on size and functionality. In the future, we plan to expand the study with other objects, include more participants, and apply our data-driven grasp type taxonomy in controlling robot grasping in our learning from demonstration framework [20], [19].

Comparing with Cutkosky grasp taxonomy, the data-driven grasp taxonomy groups the grasping motions from a different perspective. Instead of focusing on functionalities and behaviors, the data-driven grasp taxonomy provides a new insight on the grasping motion itself. Some grasp motions are

TABLE I

OBJECT MOTION GROUPING WITH DIFFERENT K'S BY k-MEANS

k	Grasp	Grasp	Grasp	Grasp	Grasp
1	Platform	Platform	Platform	Platform	Platform
2	Lateal Pinch Power Disk Light Tool Thumb-4 Thumb-3 Thumb-2 Thumb-Index Large Diamete Tripod Precision Disk Power Sphere	Lateal Pinch Power Disk Light Tool	Lateal Pinch Power Disk Light Tool	Lateal Pinch Power Disk Light Tool	Lateal Pinch Power Disk Light Tool
3	Small Diameter Adducted Thumb Medium Wrap	Power Sphere Precision Disk Thumb-4 Thumb-3 Large Diameter Tripod Thumb-2 Thumb-Index	Power Sphere Precision Disk Thumb-4 Thumb-3 Large Diameter	Power Sphere Precision Disk Thumb-4 Thumb-3 Large Diameter	Power Sphere Thumb-3 Thumb-4
4	-	Small Diameter Adducted Thumb Medium Wrap	Small Diameter Adducted Thumb Medium Wrap	Small Diameter Adducted Thumb	Small Diameter Adducted Thumb Medium Wrap
5	-	-	Tripod Thumb-2 Thumb-Index	Tripod Thumb-2 Thumb-Index	Tripod Thumb-2 Thumb-Index
6	-	-	-	Medium Wrap	Precision Disk
7	-	-	-	-	Large Diameter

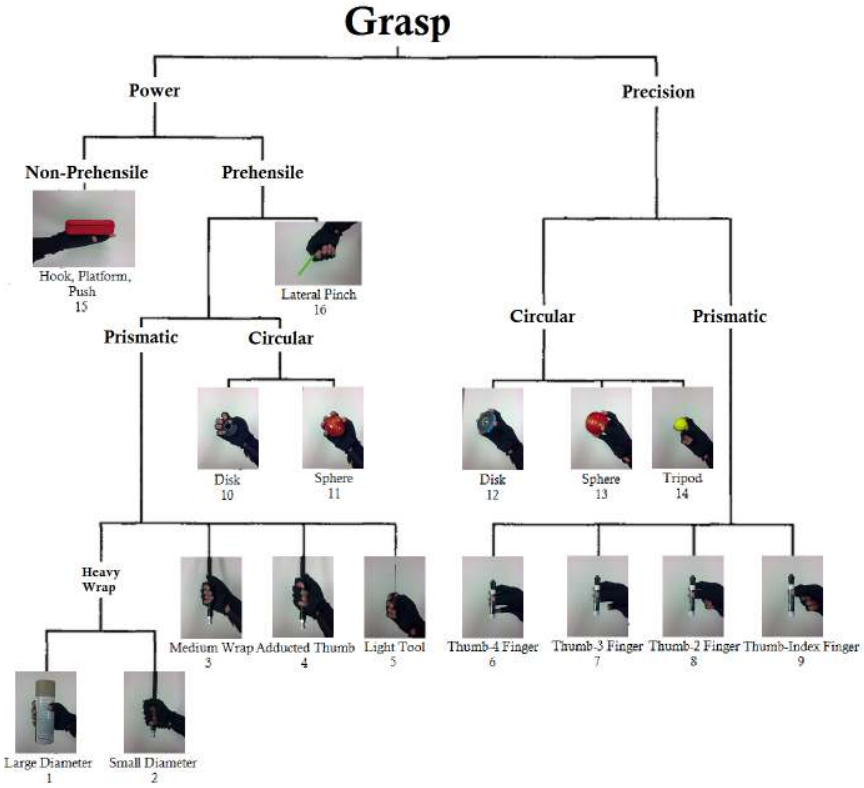

Fig. 7. Grasp taxonomy according to MARK R. CUTKOSKY [10] .

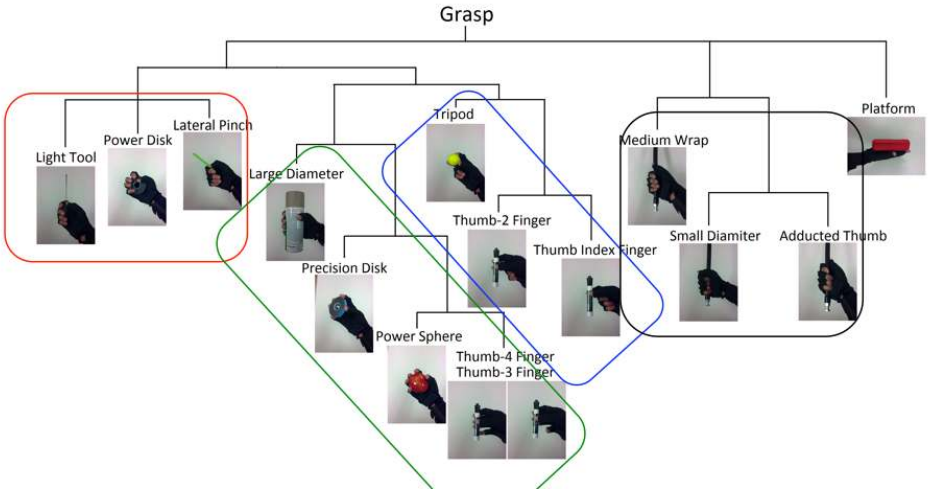

Fig. 8. Data driven grasp taxonomy according to the classification results. The four groups are indicated in blocks.

different in functionalities for its grasping objects, however, similar from the pure motion point of view and can be grouped together for motion learning, trajectory generating, and motion controller designing. Even for different grasp functionalities, but in the same data-driven grasp taxonomy group, human and perhaps a robot can apply the same motion to achieve ideal grasps and can be controlled similarly. The results also indicate that some of the grasping behaviors may have trivial differences that can be overwhelmed by the differences in the hands and styles, but the 5 grasp groups obtained by our approach are more robustly distinguishable.

ACKNOWLEDGMENTS

This work was supported partially by USF seed grant and USF Neuroscience Collaborative grant.

REFERENCES

[1] M.R. Cutkosky, R. D. Howe, Human grasp choice and robotic grasp analysis, *Dextrous robot hands* (Venkataraman ST, Iberall T, eds), pp 5-31. New York: Springer.

[2] J.F. Soechting and M. Flanders, "Flexibility and repeatability of finger movements during typing: Analysis of multiple degrees of freedom," *Journal of Computational Neuroscience*, 4: 29-46, 1997.

[3] M.H. Schieber, "Individuated finger movements of Rhesus monkeys: A means of quantifying the independence of the digits," *J. Neurophysiol.* 65:1381-1391, 1991.

[4] M. Fahrer, Interdependent and independent actions of the fingers. In: *The Hand*, R Tubiana, ed. Saunders, Philadelphia, PA, pp. 399-403, 1981.

[5] M.A. Maier, M. C. Hepp-Reymond, "EMG activation pat- terns during force production in precision grip. II. Muscular synergies in the spatial and temporal domain," *Exp. Brain Res.* 103:123-136, 1995

[6] M.H. Schieber, "Muscular production of individuated finger movements: The roles of extrinsic finger muscles," *J. Neurosci.* , 15:284-297, 1995

[7] J.R. Napier, "The prehensile movements of the human hand," *J Bone Joint Surg*, 38B:902-913, 1956

[8] N. Kamakura, M. Matsuo, H. Ishii, F. Mitsuboshi, Y. Miura, "Patterns of static prehension in normal hands," *Ame J Occup Ther* 7:437-445, 1980

[9] J.M. Elliott, K.J. Connolly KJ, "A classification of manipulative hand movements," *Dev Med Child Neurol* 26:283-296, 1984.

[10] M. R. Cutkosky, and P. K. Wright, "Active control of a compliant wrist in manufacturing tasks," *Journal of Engineering for Industry-Transactions of the ASME* 108(1): 36-43, 1986.

[11] R.L. Klatzky, J. Pellegrino, B. McCloskey, S. Doherty, T. Smith, "Knowledge about hand shaping and knowledge about objects,' *J Mot Behav*, 19:187-213, 1987.

[12] T. Iberall, G. Bingham, M.A. Arbib, "Opposition space as a structuring concept for the analysis of skilled hand movements," *Exp Brain Res*, 15:158-173, 1986

[13] M. Santello, M. Flanders, J.F. Soechting, "Postural Hand Synergies for Tool Use," *J Neuroscience*, 18(23):10105-10115, 1998.

[14] P.H. Thakur, A.J. Bastian, and S.S. Hsiao, "Multidigit movement synergies of the human hand in an unconstrained haptic exploration task," *The Journal of Neuroscience*, Vol. 28(6):1271-1281, 2008.

[15] M. Ciocarlie, C. Goldfeder, P. Allen, Dimensionality reduction for hand-independent dexterous robotic grasping, Proceedings of the 2007 IEEE/RSJ International Conference on Intelligent Robots and Systems, November, 2007.

[16] R. A. Peters and O. C. Jenkins, Uncovering manifold structures in robonaut's sensory-data state space, in IEEE-RAS Intl. Conf. on Humanoid Robots, pp. 369-374, 2005.

[17] J. Aleotti and S. Caselli, Grasp recognition in virtual reality for robot pregrasp planning by demonstration, in IEEE Intl. Conf. on Robotics and Automation, Orlando, FL, May 2006.

[18] S. Ekvall and D. Kragic, Grasp Recognition for Programming by Demonstration, Robotics and Automation, Proceedings of IEEE International Conference on Robotics and Automation, pp. 748-753, 18-22 April 2005

[19] Y. Lin and Y. Sun, Grasp Mapping Using Locality Preserving Projections and kNN Regression, IEEE Intl. Conference on Robotics and Automation, pp. 1068-1073, May 2013.

[20] Y. Lin, S. Ren, M. Clevenger, and Y. Sun, Learning Grasping Force from Demonstration, IEEE Intl. Conference on Robotics and Automation, pp. 1526-1531, May 2012.

[21] K.J. Deluzio, U.P. Wyss, B. Zee, P.A. Costigan, and C. Serbie, "Principal component models of knee kinematics and kinetics: Normal vs. pathological gait patterns," *Human Movement Science*, 16(2-3):201-17, 1997.

[22] J.O. Ramsay, B.W. Silverman, *Functional Data Analysis*, Second Edition, Springer, 2005.

[23] E. Keogh, C. A. Ratanamahatana, "Exact indexing of dynamic time warping," *Knowledge and Information Systems*, 7(3):358-386, 2005.

[24] C. Neninger, Y. Sun, S.H. Lee, and J. Chodil, A Complete Motion and Music Capture System to Study Hand Injuries among Musicians, Emergency Management & Robotics for Hazardous Environments, pp. 1-11, Knoxville, TN, Aug. 7-10, 2011,

[25] I.T. Jolliffe, *Principal Component Analysis*, Second Edition, Springer; 2002.